

# IoT enabled Intelligent Energy Management System employing advanced forecasting algorithms and load optimization strategies to enhance renewable energy generation

Challa Krishna Rao <sup>a,b,\*</sup>, Sarat Kumar Sahoo <sup>a</sup>, Franco Fernando Yanine <sup>c</sup>

<sup>a</sup> Department of Electrical Engineering, Parala Maharaja Engineering College, Berhampur, affiliated to Biju Patnaik University of Technology, Rourkela, Odisha, India

<sup>b</sup> Department of Electrical and Electronics Engineering, Aditya Institute of Technology and Management, Tekkali, Andhra Pradesh, India

<sup>c</sup> Faculty of Engineering, Universidad Finis Terrae, Providencia, Santiago, Chile

## ARTICLE INFO

### Keywords:

Renewable generation  
Energy consumption  
Load modeling  
Smart grids  
Demand-side energy management  
Machine learning  
IoT  
Energy management systems  
Forecast

## ABSTRACT

Effectively utilizing renewable energy sources while avoiding power consumption restrictions is the problem of demand-side energy management. The goal is to develop an intelligent system that can precisely estimate energy availability and plan ahead for the next day in order to overcome this obstacle. The Intelligent Smart Energy Management System (ISEMS) described in this work is designed to control energy usage in a smart grid environment where a significant quantity of renewable energy is being introduced. The proposed system evaluates various predictive models to achieve accurate energy forecasting with hourly and day-ahead planning. When compared to other predictive models, the Support Vector Machine (SVM) regression model based on Particle Swarm Optimization (PSO) seems to have better performance accuracy. Then, using the anticipated requirements, the experimental setup for ISEMS is shown, and its performance is evaluated in various configurations while considering features that are prioritized and associated with user comfort. Furthermore, Internet of Things (IoT) integration is put into practice for monitoring at the user end.

## 1. Introduction

In the upcoming years, substantial growth and concurrent challenges are anticipated in power generation, distribution, and consumption. For maximum power use, it is necessary to smoothly integrate distributed and renewable energy sources with an intelligent energy management system on the demand side. The depletion of fossil fuels and the increase interest in their reduced use in worldwide has increased the importance of renewable energy sources in response to customer demand for more reliable and reasonably priced energy. Micro-turbines for biomass, photovoltaic (PV), wind, and other renewable energy sources are becoming widely utilized [1]. Specifically, in cities, residential customers have a strong desire to install modest rooftop PV systems. The standalone PV systems necessitate substantial storage capacity while grid-connected PV systems are favored for their continuous supply over an extended period. Consequently, the need for hybrid systems, which combine the best aspects of on-grid and standalone grid systems, is growing. Many grid-connected systems, export excess power back to the

grid because of a lack of storage. In developing countries like India, this poses challenges due to grid instability and frequent outages, making the export of power back to the grid problematic [2].

## 2. Motivation and contribution

In contemporary grid-connected systems, the inclusion of PV storage has become imperative. Due to their intermittent and extremely variable character, renewable energy sources might be difficult to fully integrate into microgrids and reap their potential advantages [3]. The installation of grid-connected photovoltaic systems might exacerbate the imbalance between generation and demand, leading to overall power system oscillations. Accurate renewable energy forecast becomes essential to solving this problem.

Prioritized scheduling and storage measures are crucial for controlling consumer loads in accordance with PV energy and the utility grid's availability. For the purpose of predicting PV production, trustworthy predictive models that account for solar irradiation levels, regional

\* Corresponding author. Department of Electrical Engineering, Parala Maharaja Engineering College, Berhampur, affiliated to Biju Patnaik University of Technology, Rourkela, Odisha, India.

E-mail addresses: [krishnarao.challa@gmail.com](mailto:krishnarao.challa@gmail.com) (C. Krishna Rao), [sksahoo.ee@pmec.ac.in](mailto:sksahoo.ee@pmec.ac.in) (S.K. Sahoo), [fyanine@uc.cl](mailto:fyanine@uc.cl) (F.F. Yanine).

<https://doi.org/10.1016/j.unres.2024.100101>

Received 6 April 2024; Received in revised form 27 July 2024; Accepted 29 July 2024

Available online 8 August 2024

2666-5190/© 2024 The Authors. Publishing services by Elsevier B.V. on behalf of KeAi Communications Co. Ltd. This is an open access article under the CC BY license (<http://creativecommons.org/licenses/by/4.0/>).

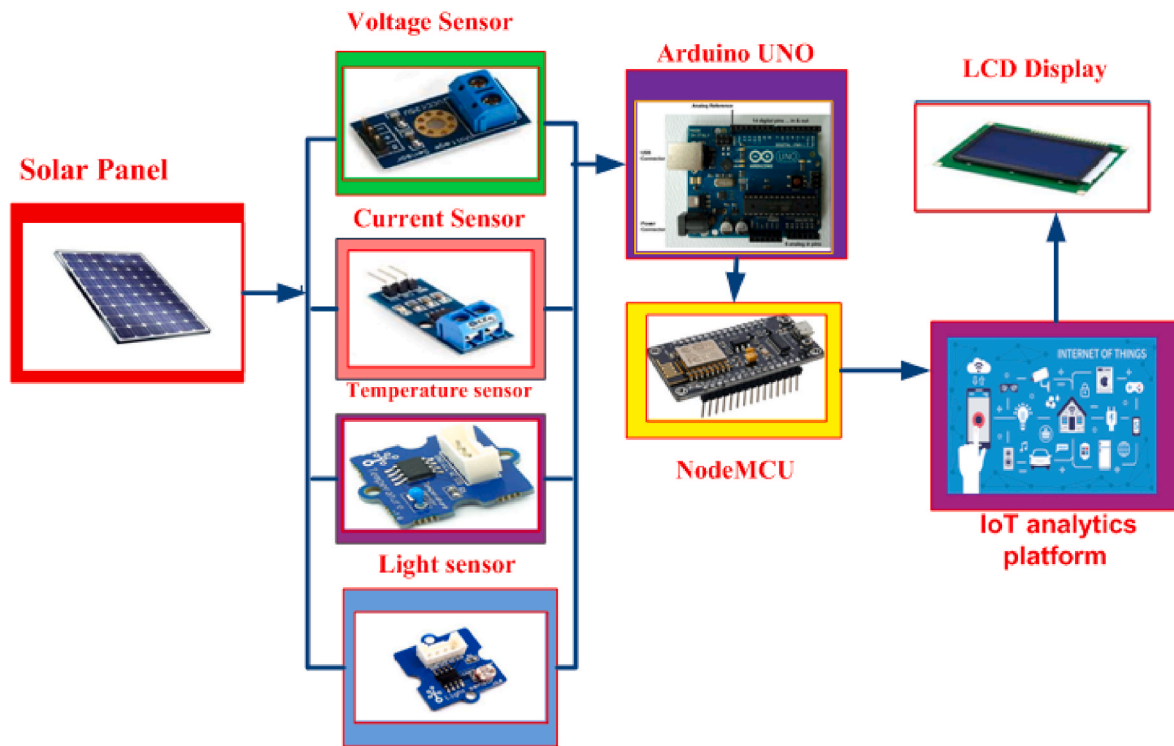


Fig. 1. Description of the intelligent energy management system [25].

weather, and other external variables must be created [4].

The presented work predominantly delves into key aspects of demand-side management, emphasizing the importance of accurate predictive models to optimize the scheduling of consumer loads in response to the availability of grid and PV energy [5].

- The study assesses a range of machine learning techniques to find reliable predictive models, such as ensemble approaches, PSO based ANN, SVM, ANN based on PSO, and Artificial Neural Networks.
- Performance metrics such as Mean Absolute Error, Root Mean Square Error and Mean Absolute Percentage Error are used to compare the generated predictive models.
- Using customizable priority options, the hardware experimental setup implements control operations in accordance with a simulated power negotiation situation based on expected power.
- The easy integration of a secure Internet of Things environment enables load monitoring and subsequent data analysis.

The Intelligent Smart Energy Management Systems architecture proposed in this study addresses demand-side energy management with an emphasis on renewable energy sources. Users may access energy administration and information in an IoT environment, and smart energy management systems plan loads using data from solar sources [6]. For both day-ahead and monthly forecasts, the machine learning technique included into the architecture allows for accurate energy forecasting. Based on the user-specified priorities, ISEMS uses the predicted data to negotiate power and transmit control actions to individual appliances [7].

### 2.1. The following sections outline the paper's organization

The literature review is built upon in Section 2, offering an understanding of the present body of knowledge and clarifying the rationale for the study undertaking. Section 3 provides a thorough review of the techniques and approaches used in this study in addition to outlining the recommended course of action. Section 4 presents the findings and

initiates a comprehensive discussion by analyzing the significance and implications of the findings. To conclude the work, the last section summarizes the key findings, offers concluding remarks, and suggests potential avenues of inquiry for further research. This final section also discusses the study's future scope and makes recommendations for new research directions and areas of study.

### 3. Literature review

Depending on considerations like location in a tropical area, surrounding circumstances, and other climatic characteristics, renewable solar PV power generation appears to be a viable and plentiful energy source globally. Nevertheless, because of its erratic and sporadic character, its reliance on factors including solar radiation, wind direction, wind speed, temperature, humidity, and daylight hours presents a problem [8]. Effectively harnessing and managing these resources becomes pivotal to meet the ever-growing energy demands of consumers. The energy industry has made tremendous advancements in the modern digital landscape with the integration of IoT environment, which allows for dependable data collection, remote monitoring, and control [9].

Due to concerns about the use of fossil fuels, independent solar PV generation is expected to play a significant role in the power sector in the near future [10]. Planning load and appliance operations at the consumer end and guaranteeing effective use depend on accurate PV output projection. Various techniques are examined to simulate sun irradiation, depending on the dataset size, factors applied, and specific usage data. Accurate renewable forecasting has the benefit of being more efficient, more affordable, and dispatchable [11]. For the purpose of ensuring the power system operates reliably, day-ahead planning utilizing demand consumption data and predictives for renewable energy is essential. Proper forecasting contributes to the preservation of system health by reducing power fluctuations and upholding overall system dependability [12].

The literature explains how to measure solar irradiance and expect energy using seasonal auto-regressive integrated moving average, radial basis function wavelet decomposition network methods, and fuzzy logic

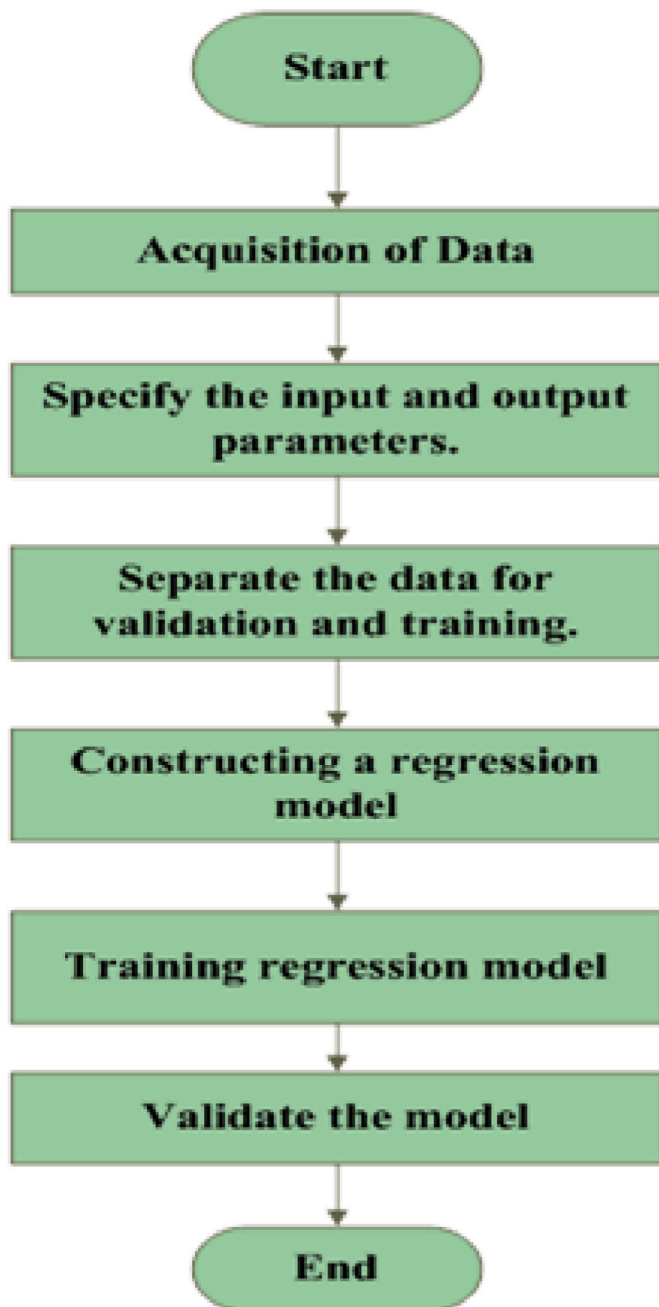


Fig. 2. A description of a primary predictive model [1].

methodologies. Furthermore, classical artificial neural network models and support vector regression have been widely used; nevertheless, parameter change significantly impacts their accuracy. Notably, recent studies explore hybrid models, ensemble methods, and support vector regression for more accurate hourly PV output forecasts [13].

The implementation of demand-side energy management systems has received a lot of attention at the same time. The literature examines Demand Response (DR) events, which let customers modify their power consumption patterns in accordance with time and utility prices to prevent peak usage [14]. In recent studies, integrated settings for managing appliance demand such as HVAC systems in commercial buildings are provided [15]. Maintaining user happiness and appliance priority is the major emphasis of several strategies for demand-side load management, predictive analysis, and optimization in energy use patterns that are examined.

The accuracy of energy meters, particularly in power measurement,

relies on the current and voltage transducers used. Experimental studies on the metrological performance of current transformers (CTs) and potential transformers (PTs), as well as the development of low-cost data acquisition-based watt-meters, have been presented in the literature [16]. Characterizing and enhancing the current and voltage transducers' metrological performance in harmonic measurement is the subject of more study [16].

This paper makes use of sun irradiation data for the Berhampur area from the National Renewable Energy Laboratory site [17]. The dataset, trained on different models, undergoes validation to assess the accuracy of prediction. Reliable source generation forecasting is considered essential for appropriate load scheduling, or pre-scheduling, in an energy management system [17]. The recommended method optimizes the parameters of the ANN and SVR models using Particle Swarm Optimization. For the provided dataset, the PSO-based parameter tuning strategy performs noticeably better than the state-of-the-art techniques [18].

The research emphasizes the need for more precise renewable energy forecast models in light of the present situation and technological developments in order to effectively control demand-side appliances without sacrificing consumer comfort. Through laboratory-level experimental settings, the advanced Smart Energy Management System of the proposed architecture is evaluated [19]. It includes a reliable communication system, an optimal load strategy, and an accurate predictive model. Furthermore, the efficiency of the energy management system is improved by the integration of an IoT environment with dynamic priority assignment that can be adjusted by the user. The gathering of large amounts of metering data opens up new research opportunities in fields like machine learning, big data analytics, real-time energy management, and energy cost optimization [20]. Numerous research groups are actively exploring these avenues to contribute to the continuous evolution of energy system management [21].

#### 4. Methodology

The Intelligent Smart Energy Management Systems design, as seen in Fig. 1, is for demand-side energy management that prioritizes renewable energy sources. The three main components of this strategy are a predictive smart energy management system, PV generation and data collecting, and an Internet of Things ecosystem that provides users with information and energy management [22]. In order to anticipate energy levels for both hourly and day-ahead scenarios, this architecture's fundamental technique uses machine learning. Based on the priority given to consumer appliances, the SEMS uses the projected information to negotiate power availability and dispatch control actions. In the context of solar energy generation, machine learning methods serve as widely adopted forecasting techniques to enhance the accuracy of the prediction [23]. This integration of machine learning into the ISEMS architecture contributes to more efficient demand-side energy management, aligning with the unpredictable nature of renewable sources [24].

##### 4.1. Design of machine learning framework

Regression analysis objective is to identify a function that, when applied to a set of input values, accurately approximates the target values. Fig. 2 illustrates the typical steps that a regression model goes through: data preparation and collection, model creation, training, and testing [26] (see Fig. 3).

##### 4.1.1. Collecting and preparing data

The initial step in designing a predictive model involves collecting a relevant dataset. The solar irradiation level data utilized in this study were based on the Berhampur area and were obtained from the NRE website (<https://nsrdb.nrel.gov>) National Solar Radiation Database Temperature, pressure, wind speed, and global horizontal irradiance are

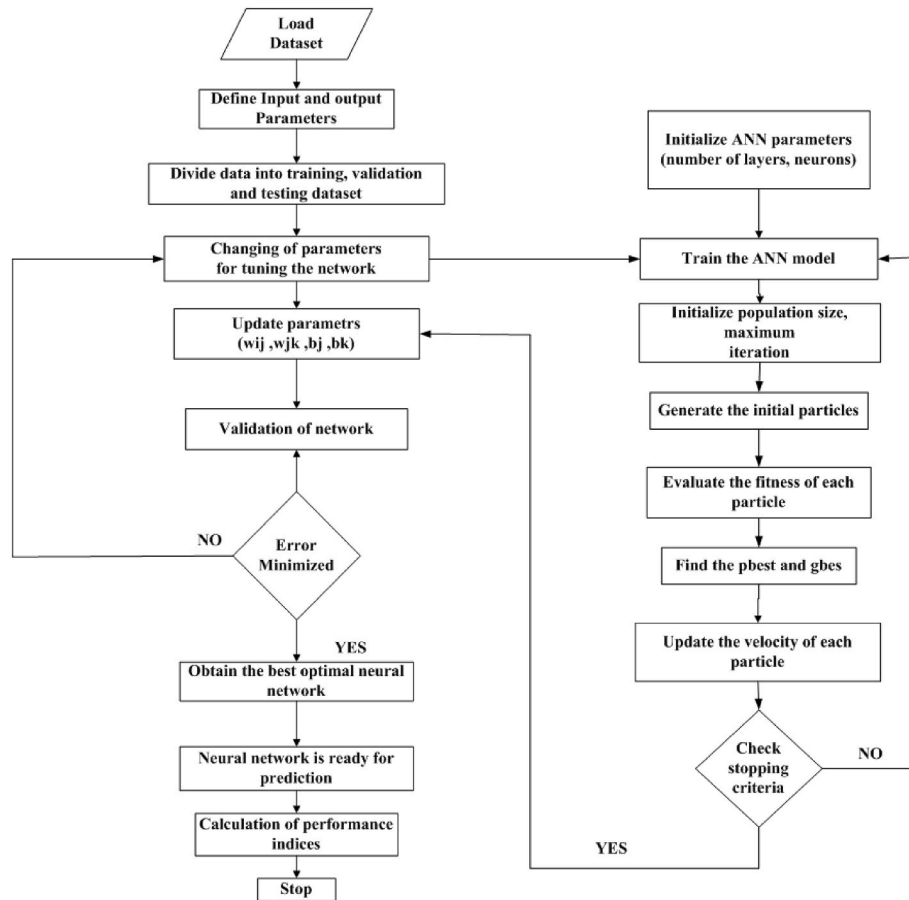


Fig. 3. ANN flowchart based on PSO [21].

the data points that are included into the regression model [27]. The missing data issue is addressed by implementing a plan to replace any missing values with the average data from the same day. Furthermore, as part of the preparation stage, the data are normalized [28].

#### 4.1.2. Creating the model

In this stage, the model's starting variables, maximum depth, and coefficients are adjusted by the designer in order to create an accurate model. The most accurate forecast model is determined by thoroughly analyzing the others. Thus, for the ISEMS forecasting approach, the PSO-based SVM regressors are considered [29].

### 4.2. Analyzing the energy management system predictive model

#### 4.2.1. Artificial neural network

An artificial neural network serves as the foundation for the traditional solar irradiation forecasting methods. An illustration of how the artificial neural network model functions using historical data with a variety of input attributes, including temperature, wind speed, day of the week, and month. Adequate data (25 %) are presented as a testing set, while the remaining 75 % was used as the training set. Finding the optimal values involves analyzing various combinations of the ANN parameters, such as the number of neurons and hidden layers. The model that is used for prediction after several trials is the one with the lowest error [25].

#### 4.2.2. ANN-based particle swarm optimization technique

The most effective parameters are determined by conducting a thorough investigation of various input parameter combinations. The first step in finding the ideal PSO (Particle Swarm Optimization) particle

size is to choose a fixed number of hidden layers ( $n$ ) and two acceleration factors ( $c1$  and  $c2$ ). To find the configuration with the least amount of inaccuracy, several combinations of variable particle sizes are taken into consideration [30]. The particle size that was found to be ideal in the first analysis is then used to calculate the ideal values for acceleration factors ( $c1$  and  $c2$ ). The concealed layer size ( $n$ ) is kept constant while doing this. To determine the ideal number of concealed layers, a third analysis is carried out in the last stage [31]. This study explores several combinations to maximize the overall performance of the model, taking into account a fixed, ideal particle size and the previously obtained acceleration factor values ( $c1$  and  $c2$ ).

#### 4.2.3. Support vector regression

Reduces training error while striking a balance in the trade-off between hyper planes compared to neural networks, logistic regression, or linear regression, Support Vector Regression (SVR) employs a distinct approach for optimization. The meta-parameter Gamma is crucial because it defines the Gaussian kernel function, evaluates the degree of similarity between different qualities, and assigns weights to the optimization functions that correspond to those features. Moreover, regularization parameter C carries out the subsequent tasks [32]:

The SVR model's hyper parameters are initially set randomly and derived from the data pattern. The accuracy of the model hinges on the values assigned to these parameters, and for the SVR model, an initial setting of Gamma = 1.25 and C = 1 is employed. The subsequent section delves into the optimization algorithm used for fine-tuning these parameters [33].

#### 4.2.4. Support vector regression based on PSO

The SVR model's predictive accuracy depends on determinants out

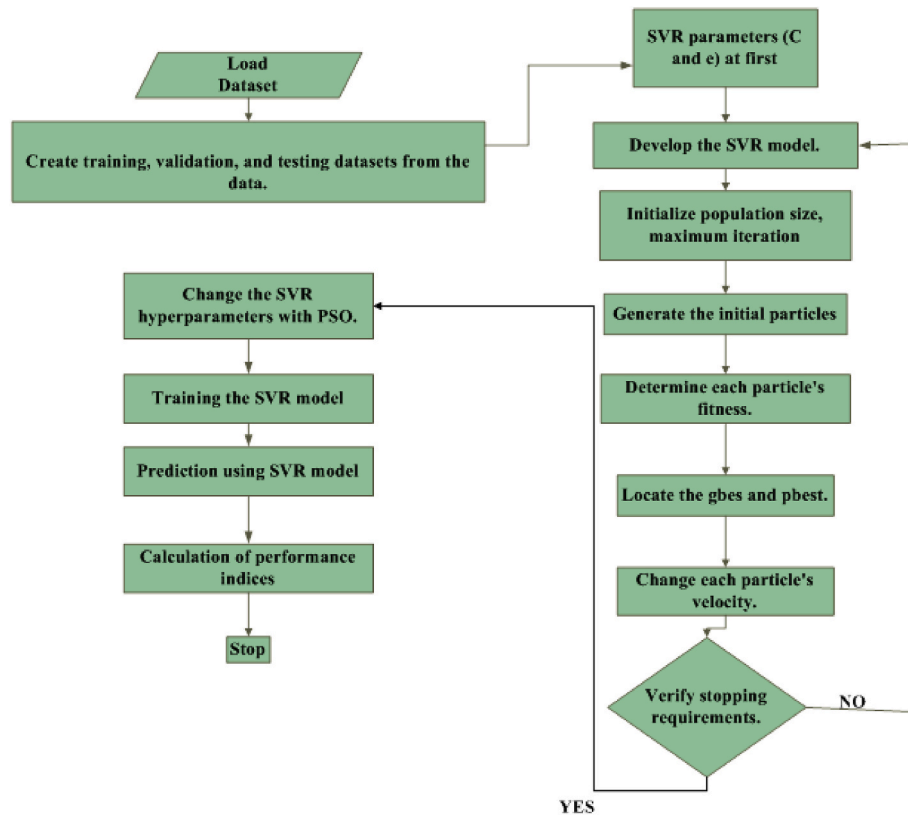


Fig. 4. PSO based SVR flowchart [9].

what the ideal values for the C and Gamma parameters are. An efficient method for maximizing these SVR parameters is Particle Swarm Optimization. In order to find the lowest predictive error possible throughout the whole solution space, PSO-SVR evaluates the SVR model's predictive error in each iteration in a methodical manner. Next, the best values for the SVR parameters that are being studied are determined using this information [34].

The flowchart in Fig. 4 illustrates how the PSO-SVR model operates. The SVR function initially sets random values for the SVR model's hyperparameters. Random indexing, a technique covered in the preceding part of this chapter, is used to split the dataset into training and testing lists. Next, in accordance with the PSO's requirements, the SVR technique is used frequently. Performance evaluation of the model is done at each iteration minimizing error is the goal of PSO's iteration direction selection process [35].

The PSO determines the best solution as the collection of hyper parameters that correspond to the least error value. After making this decision, the model is used to forecast using the testing data and the best hyper parameter configuration.

#### 4.2.5. Ensemble methods

In data analytics, feature collection is crucial, and Decision Tree methods provide a noteworthy benefit by fitting the dataset with feature selection implicitly. Unlike certain regression models that require proportional scaling among parameters, decision trees demand minimal effort for data preparation. Further, they exhibit remarkable performance in handling nonlinear relationships between parameters without necessitating linear assumptions. In this particular study, basic learners are chosen by a series of iterative trials based on trial and error [36]. This method achieves a greater accuracy rate while simultaneously using less computing power. When compared to other standard techniques, the ensemble of decision trees performs better.

#### 4.3. Predictive performance evaluation metrics

One important factor in deciding if the trained model is suitable for real-world applications is performance evaluation. In this study, three key performance criteria are thoroughly examined to gauge the accuracy of the model. These three performance metrics are.

- Mean Absolute Percentage Error
- Mean Absolute Error
- Root Mean Square Error

All of these performance indicators add up to a thorough assessment of the model's efficacy, providing information on its accuracy and dependability for real-world applications [37].

##### 4.3.1. The mean absolute error

The forecast error is the difference between the actual and predictable data values, and it is calculated using Mean Absolute Errors (MAEs). The average absolute gaps between each expected value and its matching actual value are measured by this statistic. Using MAEs gives the assessment process a clear indicator of the forecasting performance overall and provides insights into the forecasting model's accuracy and precision [38].

$$MAE = \frac{1}{N} \sum_{i=1}^N |\vec{P}_i - P_i| \quad (1)$$

##### 4.3.2. The mean absolute percentage error

A statistical indicator called Mean Absolute Percentage Error or Mean Absolute Percentage Deviation is used to assess the accuracy of forecasting techniques, particularly with regard to trend predictive. MAPE is often stated as a percentage and may be calculated using the following formula [38]:

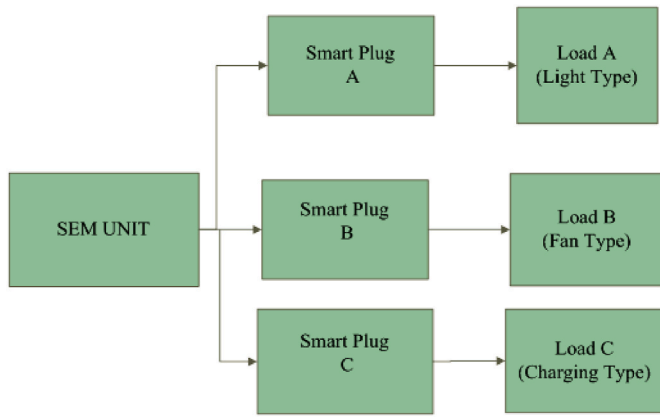


Fig. 5. Intelligent energy management system [31].

statistic takes into consideration the size and direction of each individual error when calculating the mean error magnitude. The RMSE is calculated using the formula below

$$RMSE = \sqrt{\frac{1}{N} \sum_{i=1}^N \frac{|\vec{P}_i - P_i|^2}{P_n}} \quad (3)$$

For the produced models, several trials and combinations are used to carry out detailed analysis.

### 5. Analysis of the ISEMS experimental design

This section provides an overview of the Intelligent Smart Energy Management System’s experimental setup. It describes the smart socket’s architecture in depth and clarifies the power negotiation algorithms that are essential for effective energy management. Subsequently, the integration of IoT framework with ISEMS is detailed, emphasizing its role in facilitating remote monitoring of data. This comprehensive description aims to offer insights into the structure and functionality of the ISEMS experimental setup, encompassing both hardware and algorithmic components [39].

#### 5.1. The configuration of the overall system

The complete Smart Energy Management system, seen in Fig. 5, consists of a smart socket module and a SEM unit. The brains of the system are the SEM Gateway and the smart socket module, which controls the connected appliances. XBee modules provide bidirectional communication between the SEM Gateway and the smart socket module. In the configuration, these modules act as a router at one end and a coordinator at the other. The brain of the system, the SEM unit, completes power negotiation algorithms and then, upon receiving external signals, transmits control signals to the smart socket module. The next section goes into further depth about appliance planned operations based on projected power statistics [40]. Real loads are used in the lab’s experimental system, including a laptop that has to be charged, a fan, and illumination. Algorithms established in the SEM unit are used to sequence the appliances’ actions during Demand Response (DR) events based on predetermined priorities. In order to schedule appliances in accordance with the Time of Usage and stay under the minimum slab

$$MAPE = \frac{1}{N} \sum_{i=1}^N 100 \frac{|\vec{P}_i - P_i|}{P_n} \quad (2)$$

The number of test points in this instance is N, the nominal power is P<sub>n</sub>, the actual value at the i<sup>th</sup> hour is P<sub>i</sub>, and the predicted value is P̄<sub>i</sub>.

The Mean Absolute Percentage Error (MAPE) offers two distinct advantages in the context of forecasting evaluation. First, by utilizing absolute values, it stops the cancellation of positive and negative mistakes. This ensures that the measure accurately reflects the magnitude of the errors, without any offsetting effects.

Second, the benefit of MAPE is that the size of the dependent variable has no bearing on relative errors. This characteristic allows for a meaningful comparison of forecast accuracy across datasets with different scales. In project work, placing primary importance on MAPE acknowledges its ability to provide a reliable and scale-independent assessment of forecasting accuracy, contributing to a more robust evaluation of the model’s performance.

#### 4.3.3. Root Mean Square Error

An estimator or model’s predicted values and the actual observed values are typically compared using a metric called Root Mean Square Deviation, often known as the Root Mean Square Error [38]. This

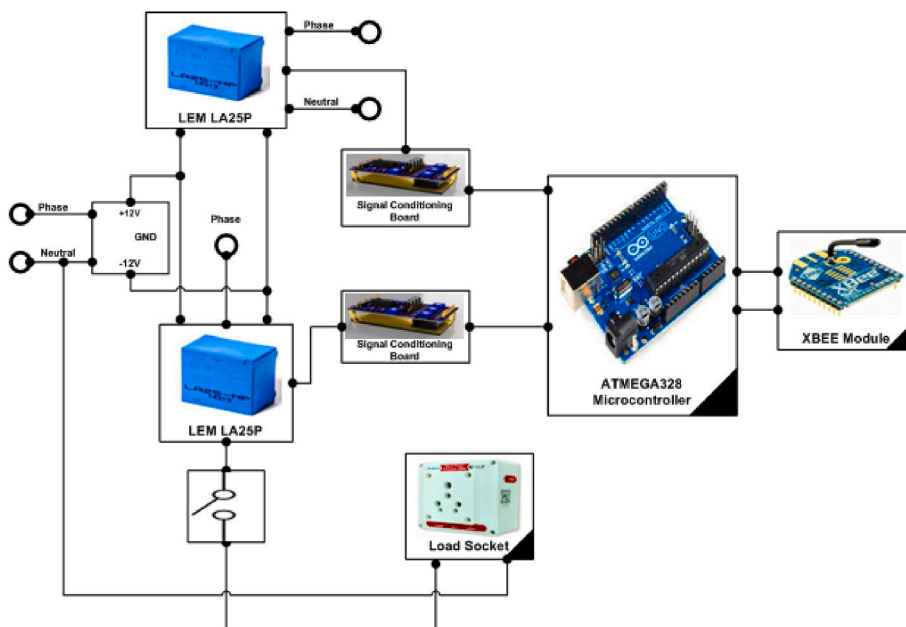


Fig. 6. Designing a smart socket for an intelligent energy management system [34].

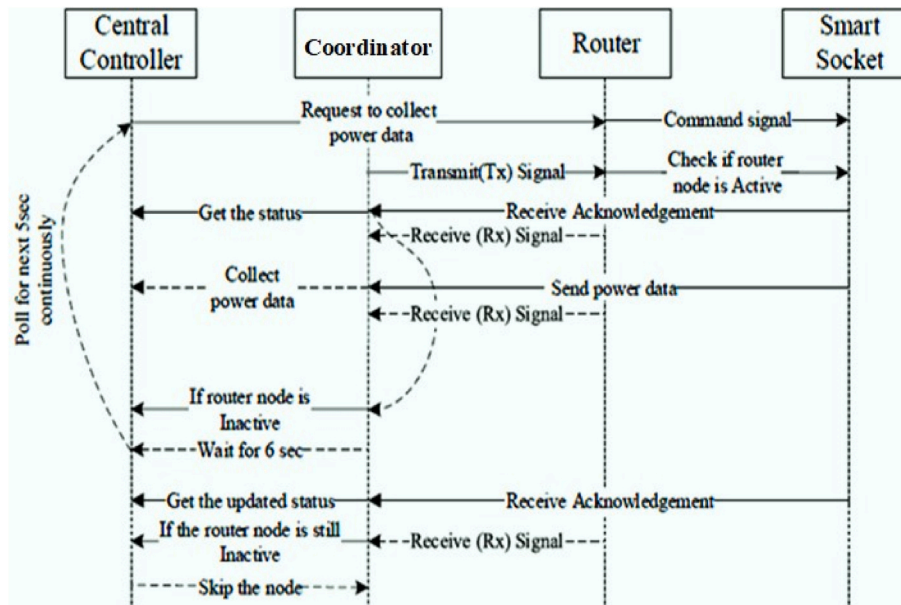


Fig. 7. An algorithm characterized by decisive decision-making capabilities alongside self-diagnostic functionality [38].

rate, the system takes into account the maximum demand limit. This strategy guarantees effective resource management and energy management.

In the laboratory, actual loads are used to replicate real-world conditions in the experimental setting. Load-A specifically refers to an incandescent lighting load. This load is equipped with the capability to vary power consumption by toggling the status of individual bulbs within it. Load-B in the setup is represented by a fan. This fan is equipped with temperature and humidity sensors and can change its speed. This integration showcases how user comfort considerations are incorporated into the algorithms deployed within the Smart Energy Management System (SEMS). The Load-C is exemplified by a charging laptop, deliberately chosen to illustrate the scheduling of chargeable loads with a focus on Time of Usage [41]. This intentional selection emphasizes the system's ability to optimize the operation of devices based on predetermined time intervals, contributing to efficient energy utilization. Together, these loads provide a diverse and comprehensive test for evaluating the SEMS algorithms in a controlled laboratory environment.

### 5.2. Smart socket design for ISEMS

The schematic design of a smart socket, as seen in Fig. 6, uses Hall Effect voltage and current transducers to convert single-phase power characteristics (voltage and current) into low-level voltage signals. The input resistance  $R_1$  in the voltage transducer scheme (Fig. 6) is selected to guarantee that the measurement resistance  $R_M$  is between 10 and 350  $\Omega$ . In a similar vein, a measurement resistance ( $R_M$ ) is incorporated into the current transducer circuit (Fig. 6) to guarantee that the output voltage stays below 4.5V. A voltage divider circuit used by the power supply module to create a 1.8V DC offset is one of the signal conditioning circuits that further refines these signals. A Zener diode with a 4.7V cut-off voltage is included in the signal conditioning circuit to guard the Arduino microcontroller and prevent over voltage [42].

The Arduino microcontroller's analog pins receive the output signals after they have been conditioned within the 0–4V range. Based on instructions received from the microcontroller, the relay module permits the turning on or off of a certain appliance. By attaching the SEMS unit (Router) to the smart socket, an XBee Series 2 module creates the communication channel. Every load controller has access to control commands transmitted by the SEMS unit. Through Xbee modules, the

Arduino in the coordinator module receives orders from various routers and SEMS units. It is in charge of gathering information on energy usage from every router and providing users with an LCD interface to view statistics on total energy use. The Arduino Ethernet shield may be used to upload this energy usage data to the local server (WAMP). The SEMS can effectively manage energy thanks to the integration of sensor, control, and communication components in the smart socket design [43].

### 5.3. Predictive power data driven algorithmic decision-making

When the generated power is insufficient to meet the whole demand, users may still operate their priority appliances thanks to an algorithm included into the SEM hardware. This algorithm takes into account the consumer-assigned priorities to different appliances. The available power during the demonstration is assumed to come from solar PV output, which is estimated using the anticipated sun irradiation. This predictive approach enables the SEM system to allocate generated solar power efficiently, allowing consumers to use their most essential appliances, taking into consideration individual priorities [44]. The algorithm ensures optimal utilization of available solar energy, enhancing flexibility and user satisfaction within the SEMS.

#### 5.3.1. Demand Response involves the use of a decisive algorithm

**Algorithm 1.** provides a detailed walkthrough of the deployed algorithm, outlined as follows:

The first step in the SEM decisive approach is to collect power use data from each device in a predetermined sequence. The next part explains the self-diagnostic process that the SEM unit executes in the event that a load controller fails to provide the required data [45]. Consumer priorities are used to arrange the collected power usage statistics. The SEM unit next looks over the information to see if any demand limit breaches may have occurred. This last algorithm examines if the apparent power used by appliances is more than the specified maximum demand limit [46].

In order to maintain the demand limit from being exceeded, for the purpose of turning on the greatest number of high-priority appliances, the SEM unit sends out command signals. The remaining appliances are turned off simultaneously by sending out command signals [47]. The algorithm scrutinizes activated appliances to confirm the presence of peak load conditions. This criterion is fulfilled upon receipt of a peak

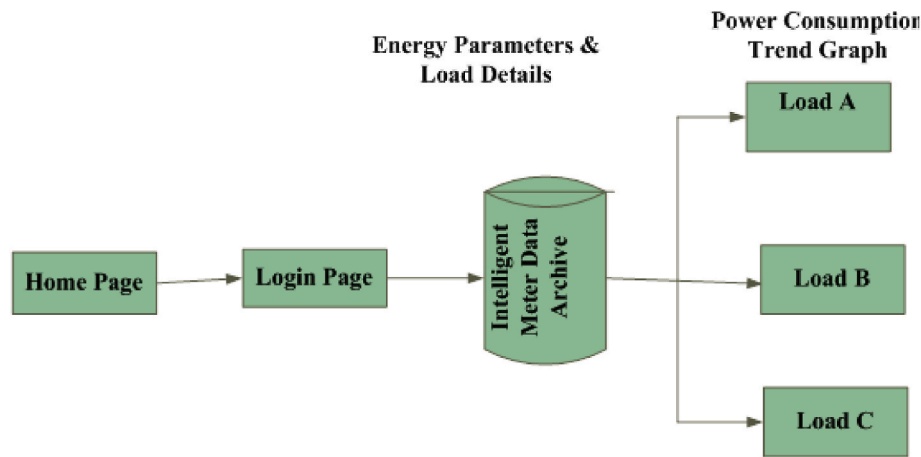


Fig. 8. An overview of the Internet of Things [50].

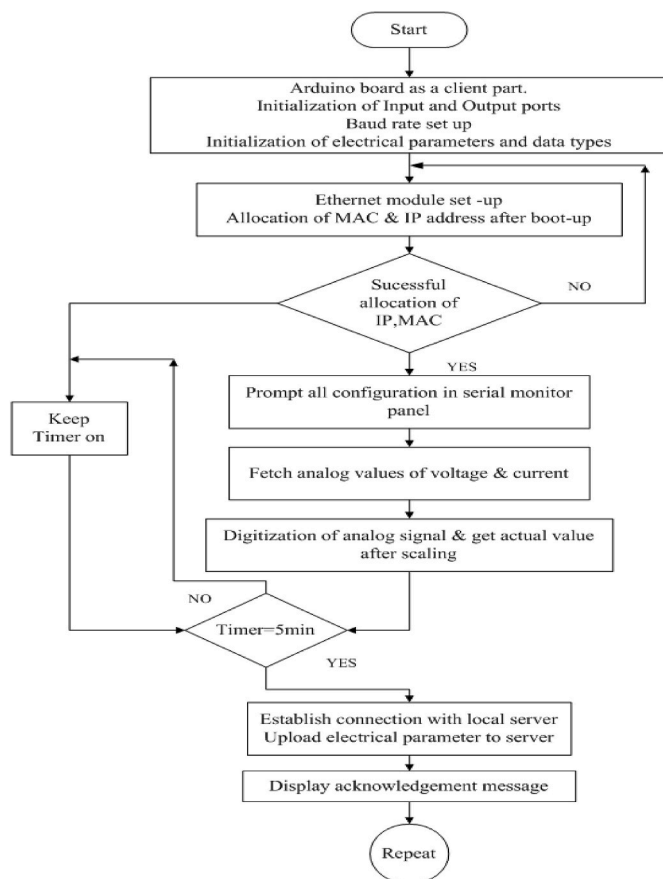


Fig. 9. Developing firmware for the IoT infrastructure of an Intelligent Energy Management System

load hours signal from the utility, in addition to the appliance’s apparent power exceeding 25 % of the highest apparent power consumption recorded for the home in the preceding month [48]. In order to prevent potentially expensive tariff charges, the SEM unit notifies the load controller of increased power usage during peak load hours when the peak load criteria is fulfilled. The load controller then sounds an alarm to the customer by turning on the LED and buzzer for 1 s [49].

When the appropriate command signals are sent to every device, the SEM unit waits 30 s before initiating the subsequent data sampling cycle. Customers are able to swap out the appliances that are given priority

during this time. After that, repeat steps 1 through 6 to complete the process again. The flow chart for the SEM decisive technique for ‘n’ number of loads within a house is shown in Fig. 2. Emphasize that appliance priorities are initialized with preset values before this procedure is run [50]. To collect data on power consumption from all appliances, the flow chart also uses two variables, “i” and “k,” where “i” increments based on priority and “k” increments in a predefined sequence.

#### 5.4. Energy monitoring system integrated into an IoT environment

Energy usage may be monitored in real time in a residential complex with smart meters. When an Ethernet shield manages a successful connection, the SEMS enables the smooth flow of power data to a server. The uploaded data may be viewed and accessed by data monitoring systems and devices, as Fig. 7 clearly illustrates. Designed for gathering and monitoring data in real-time, the local host monitoring system comprises of a server and database management system [51]. The server runs within the local network (intranet) and is powered by the WAMP stack (Windows, Apache, MySQL, and PHP). The power settings of the server may be accessed via the Internet by changing its hostname from local host to a certain domain name. The server is configured with many databases to hold different power settings [52]. Fig. 8 shows the firmware, which is in charge of creating a connection and uploading data. Every 5 min, power data is transmitted to the server. Only authorized users who have successfully authenticated using their credentials are permitted access to the online site. The subsequent section presents results and trend graphs derived from the uploaded power data [53] (see Fig. 9).

## 6. Results and discussion

This section explores the Intelligent Smart Energy Management System’s validation as well as the demand-side consumer-focused forecast outcomes. The most accurate predictive system has been determined by a thorough investigation of many machine learning models. The experimental setup, detailed in the prior section (Section 4), is implemented, and diverse scenarios are illustrated to showcase optimal load scheduling based on assigned priorities, taking into account the predicted power values. IoT ecosystem is integrated for thorough data monitoring and analysis as the process comes to a close. Through this connection, the system’s real-time data monitoring and analysis capabilities are improved, guaranteeing an adaptable and flexible approach to energy management.

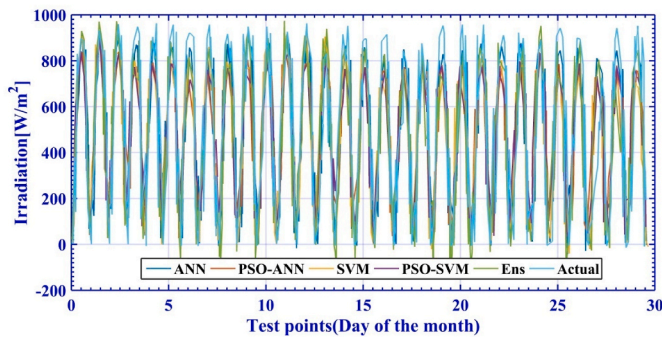


Fig. 10. Forecasting sunny days in April using various predictive models

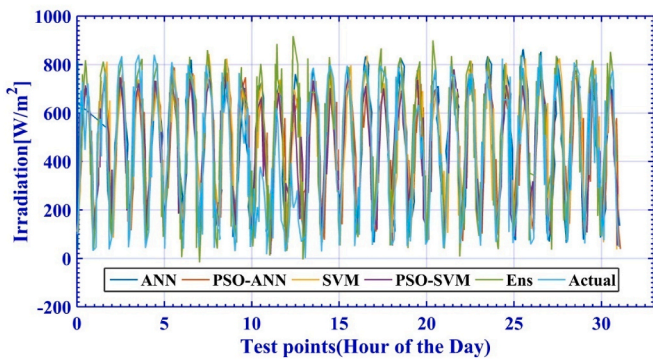


Fig. 11. Forecasting winter days in December using various predictive models

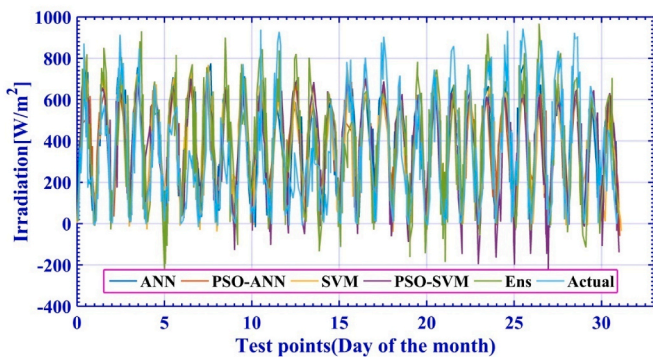


Fig. 12. Predicting rainy days in July using diverse predictive models

### 6.1. Analyzing forecasting models

This phase does a study of the data using several machine learning models in order to determine the most accurate predictive technique. In order to guarantee accuracy in the models, the method of parameter tuning is investigated to identify ideal values. The created models are used to provide month- and day-wise forecasts, providing detailed insight of performance across many temporal scales. The optimal-performing model is then identified by a comprehensive error analysis that follows. In order to improve the Intelligent Smart Energy Management System’s forecasting accuracy and dependability, a thorough analysis is being conducted to improve the system’s predictive potential.

#### 6.1.1. Tuning the parameters of optimization methods

Parameter tuning is the practice of experimenting with various combinations to use the optimization technique to find the most effective optimal value. A brief summary of the parameter tuning processes for several algorithms is provided below.

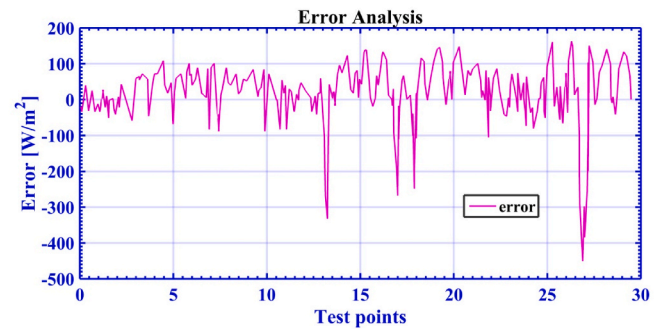
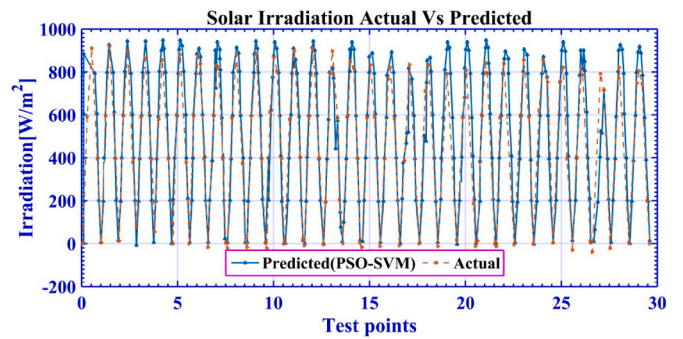


Fig. 13. Forecast for sunny days in April based on PSO SVM model, categorized by month

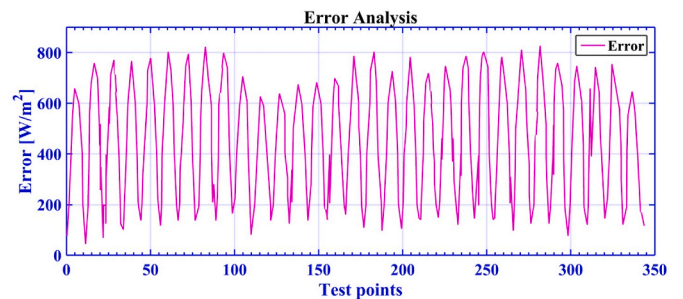
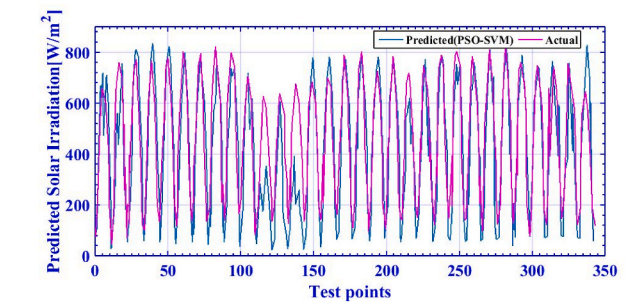


Fig. 14. Predictive for winter days in December, segmented by month, using the PSO SVM model

6.1.1.1. *Parameter tuning of support vector regression.* In a standard SVR algorithm, hyper parameters are conventionally chosen randomly. However, this study employs Particle Swarm Optimization (PSO) as a general optimization algorithm to pinpoint optimal values for SVR parameters. PSO looks for the optimal point methodically over the whole solution space. By using PSO to intelligently walk through the solution space without having to look at every point; this method drastically cuts down on the amount of time needed to achieve optimal values.

6.1.1.2. *Parameter tuning of artificial neural network.* An artificial neural network has a variable number of neurons in the hidden layer, an

**Table 1**  
Analysis of errors on a month-wise basis.

Month	Error	ANN	SVM	ANN based PSO	SVM based PSO	Ensemble
December	MAE	68.2352	82.9758	66.6141	61.5253	81.7439
	MAPE	6.82352 %	8.29758 %	6.66141 %	6.15253 %	8.17439 %
	RMSE	109.2051	116.4047	120.6795	110.7607	139.9101
April	MAE	71.3958	75.6092	69.9437	62.7569	76.6585
	MAPE	7.13958 %	7.56092 %	6.99437 %	6.27569 %	7.66585 %
	RMSE	92.9088	115.4521	119.5849	84.8527	101.8459
July	MAE	127.9802	129.9028	127.288	116.7738	131.7008
	MAPE	12.79802 %	12.99028 %	12.7288 %	11.67738 %	13.17008 %
	RMSE	166.6358	163.8629	192.4353	158.8484	202.5224

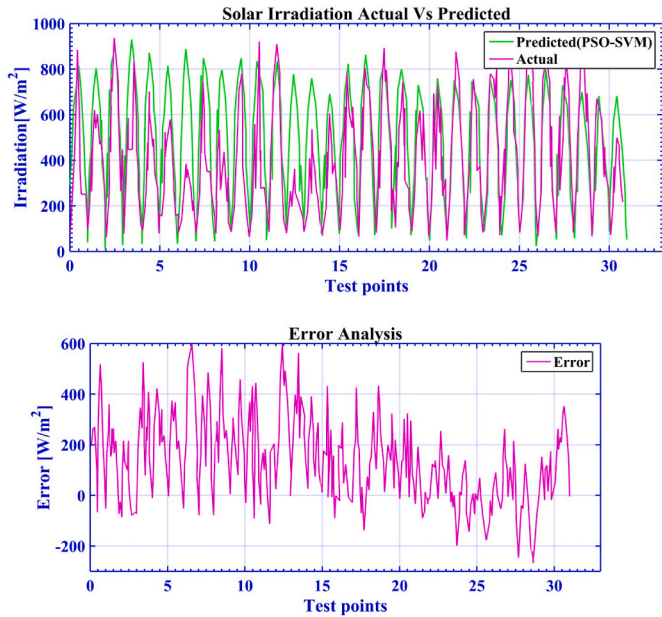


**Fig. 15.** PSO SVM model-based forecast for rainy days in July, organized by month

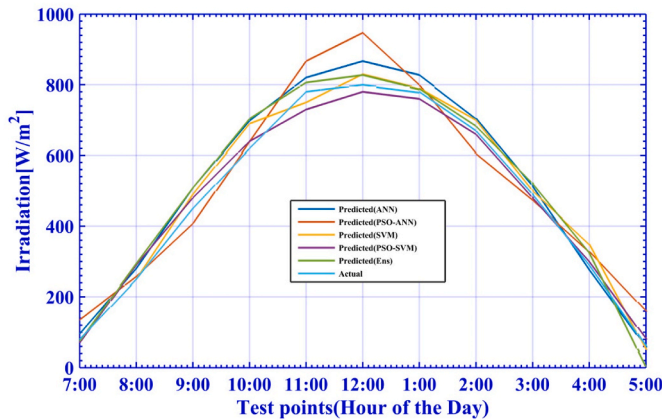


**Fig. 16.** Forecasting power levels on a day-to-day basis using various models

independent number of inputs, and a dependent number of outputs. PSO is used to optimize a number of variables, including swarm population size (N), inertia weight (w), and acceleration factors (C1 and C2). The number of neurons (n) in the hidden layer during this waiting period is the ANN parameter. It is common practice to choose the inertia weight at random.

There are other ways to choose the number of hidden layers, acceleration factors, and size of the swarm population. The experiment

**Table 2**  
Device state of operation behind Load arrangement.

Devices	Device status	Priority	VA Power (kW)	Power Demanded (kW)	MDL (kW)	Device position
Load-A	Turn on the Switch (one Light)	High	0.02	0.185	0.196	Turn on the Switch
Load-B	Turn on the Switch	Medium	0.08	0.185	0.196	Turn on the Switch
Load-C	Turn on the Switch	Low	0.085	0.185	0.196	Turn on the Switch

**Table 3**  
Device state of operation behind Load arrangement.

Devices	Device status	Priority	VA Power (kW)	Power Demanded (kW)	MDL (kW)	Device state of operation
Load-A	Turn on the Switch (Two Light)	High	0.04	0.205	0.196	Turn on the Switch
Load-B	Turn on the Switch	Medium	0.08	0.205	0.196	Turn on the Switch
Load-C	Turn on the Switch	Low	0.085	0.205	0.196	Turn off the Switch

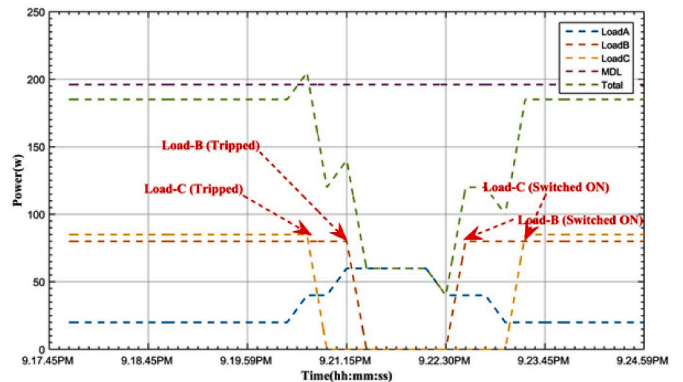


**Fig. 17.** Scheduling loads according to their assigned priorities

**Table 4**  
Device state of operation following Load arrangement.

Devices	Device status	Priority	VA Power (kW)	Power Demanded (kW)	MDL (kW)	Device state of operation
Load-A	Turn on the Switch (3 Light)	High	0.06	0.225	0.196	Turn on the Switch
Load-B	Turn on the Switch	Medium	0.08	0.225	0.196	Turn on the Switch
Load-C	Turn on the Switch	Low	0.085	0.225	0.196	Turn off the Switch

comprises changing the number of hidden layers (n) and the acceleration factors (C1 and C2) while keeping the swarm size constant. Next, using the previously established optimal swarm size and the same hidden layer size (n), the ideal values of the acceleration factors (C1 and C2) are calculated. In order to determine the optimal value, the final analysis looks at several combinations of C1, C2, swarm population size, and hidden layer topologies while accounting for the ideal swarm size and acceleration factor values (C1 and C2).

**6.1.2. On a monthly basis seasonal forecasting with machine learning methodology**

Historical data provide yearly insights into the Berhampur region’s monthly seasonal forecast, allowing the months to be divided into wet, summer, and winter seasons. The statistics showed that significant rainfall occurred in June, July, August, September, and October, with July being the wettest month. In addition, it was discovered that December was the coldest month and May was the warmest.

The simulation studies included five distinct predictive models: ensemble techniques, SVM, PSO-SVM, ANN, and PSO-ANN. In separate tests, the models were trained using the 2021 and 2022 datasets to estimate predictive accuracy, and then they were validated using the 2022 dataset. The predictive models performance was assessed using a variety of assessment criteria, including MAPE and MAE. Remarkably, in bright conditions, the PSO-based SVM model performed better than other models.

Similarly, simulation experiments for winter days utilized training data from 2020 to 2021, with testing on December 2022 data, as illustrated in Fig. 10. Although solar irradiation levels were lower than during sunny days, the periodic nature of irradiation contributed to enhance predictive accuracy, with the PSO-based SVM model demonstrating superior performance. Finally, simulation experiments for rainy days involved training data from 2020 to 2021, with testing on July 2022 data, as illustrated in Fig. 11. Rainy days exhibited lower and more erratic solar irradiation levels, leading to a notable increase in error rates. The PSO-based SVM model consistently performed better than the other approaches examined. Concluding the analysis, Fig. 12 showcases the April month predictive for the PSO-based SVM model during the summer season, along with error metrics. The comprehensive experimentation and comparison across seasons highlight the effectiveness of the PSO-based SVM model in accurately predicting solar irradiation

**Table 5**  
Analysis of power consumption within the ISEMS.

SEM element	Apparatus	The approximate amount of power used	Duration of Operation	Total Annual Energy Use (kWh/year)
SEM Device	Xbee chip microcontroller with 16*2 LCD display and Ethernet shields.(Data transfer occurs every minute.)	0.1856 W	operates around-the-clock and displays energy on an LCD screen	1.801
Load Controllor	Module for sensors and power supply small controller Zigbee component Switches	0.8492 W	operates around-the-clock and displays energy on an LCD screen	7.547

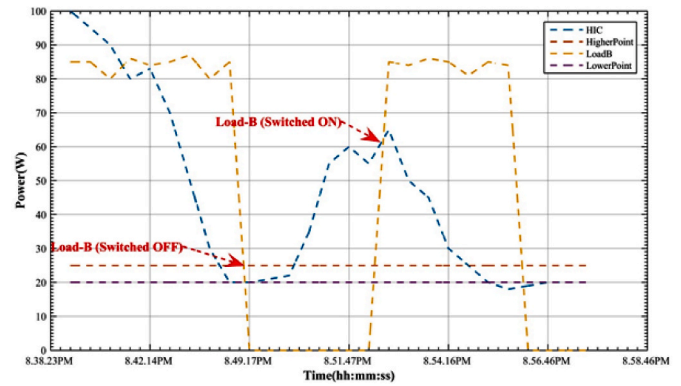


**Fig. 18.** Scheduling loads based on sensed parameters

levels in the Mangalore region.

Figs. 13 and 14, respectively, provide error analysis plots for the winter and summer seasons. Table 1 offers a thorough month-by-month comparison using several assessment measures. The PSO-based SVM model outperforms all other regression models, as seen by Table 1, particularly in terms of mean absolute percentage error. It’s interesting to note that the ANN and Ensemble techniques exhibit better accuracy in December and April as well because these are the months when the data is more periodic. However, challenges arise in July, the rainy season, where historical data is characterized by significant randomness, posing difficulties in accurate predictives. Despite these challenges, the PSO-based SVM model demonstrates superior performance across diverse seasonal conditions, affirming its reliability in predicting solar irradiation levels in the Mangalore region.

**6.1.3. On a daily basis forecasting using a machine learning method**

A comparison of many machine learning-based regressors for forecasting solar irradiance on a given day is shown in Fig. 15. The graphic shows the time (in hours) and the amount of solar radiation, covering the hours of 7 a.m. to 5 p.m. After being trained on a two-year dataset extracted from the NSRDB database, the model performance was assessed daily. Remarkably, among all the implemented forecasting regressors, the PSO-based SVM regressor emerges as the top performer, as highlighted in Fig. 15. This underscores the robustness and efficacy of the PSO-based SVM model in accurately predicting solar irradiance levels throughout the course of a day, showcasing its superiority over alternative techniques in this specific context.

**6.2. Analysis of ISEMS efficiency**

This section contains the findings of these experiments from the several situations that have been presented and analyzed. In order to demonstrate the efficacy of the energy management system through user comfort scenarios and cost optimization strategies, the trials run in which varying orders of priority are assigned to appliances with unique configurations. To assess the performance of the energy management system, different priority configurations were assigned to appliances, reflecting varying levels of importance. Additionally, scenarios were

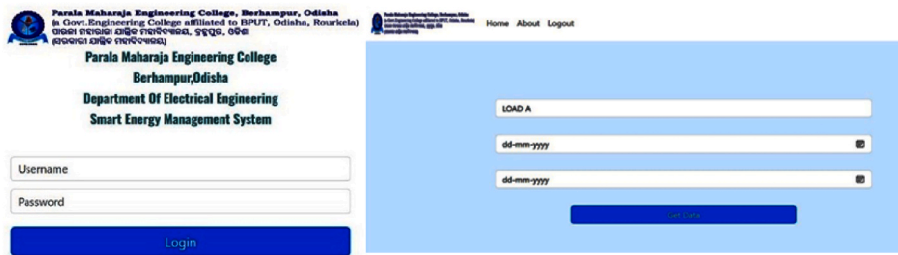


Fig. 19. Web access interface and power consumption

explored that where related to user comfort, aiming to optimize energy consumption while ensuring a satisfactory user experience. Cost optimization techniques were employed to further demonstrate the efficiency of the energy management system in achieving economical energy consumption patterns.

The results obtained from these experiments provide valuable insights into the system's adaptability to diverse scenarios and its ability to balance user comfort with energy efficiency. The analysis of these results sheds light on the effectiveness and versatility of the energy management system, affirming its potential in real-world applications.

#### 6.2.1. Load operation strategy with specified priority using available power

The bank of incandescent bulbs in this particular case is called Load A and is given the greatest priority, followed by a fan load that is given a mid-priority. Due to its schedule ability, the battery charging load is assigned a low priority. The load scheduling function of the Smart Energy Management system is shown in Fig. 16. The maximum demand (the input from the utility) is set at 196W in Fig. 16. Due to the fact that the overall power usage stays within the Maximum Demand Limit (MDL), or available power, all three loads are operating from 9.17.45 p.m. to 9.20.45PM. Two incandescent lamps are turned on at 8:19:44 p.m., which raises the overall power usage above the MDL. In response, the SEM controller quickly turns off the battery charging load. Afterwards, at 9:20:45 p.m., an additional bulb (three lights on) is turned on, increasing the lighting load's power usage. To keep supply and demand in balance, the controller, however, disables the second load because the lighting load alone uses 185W of the 196W MDL.

Table 2 under case (1) provides a summary of the appliance scheduling by SEM in this instance, along with comprehensive power usage data. Altering the load priority order has an impact on the appliance state after load scheduling, as Table 3 illustrates; this is also noted in the same table under instance (2). These cases exemplify the adaptability of the SEM system in managing diverse load configurations and priorities effectively.

#### 6.2.2. Establishing user preferences using data collected

The SEMS includes a temperature and humidity sensor (the DT H11 module) to improve user comfort. Fig. 17 shows the features of load scheduling dependent on temperature and humidity. The recommended SEMS allows users to freely select the lower and higher threshold criteria for room temperature. The SEMS turns on the fan load controller in accordance with the room temperature when it rises over these set limits. The room temperature in Fig. 17 drops below 22 °C at 08:44:21 p.m., causing the controller to turn off the fan load. The controller then triggers the fan load at 08:52:17 p.m. because the temperature has risen over the upper limit of 25 °C. This integration of temperature and humidity-based load scheduling ensures that the SEMS not only optimizes energy consumption but also prioritizes user comfort by adjusting loads based on environmental conditions. The system's responsiveness to temperature fluctuations exemplifies its capability to provide a personalized and comfortable environment for users.

#### 6.2.3. Calculating accuracy and measuring power consumption of ISEMS units

One specific power meter that is recognized as the industry standard is used for calibration in this study. Here is the formula used in the calibration process:

(Measured value - offset factor) \*k = (Value observed in ref power meter)

Here, k stands for the scaling factor. For more than two load scenarios, the power levels are recorded from both the reference meter and this study's using configuration. The scaling factor and offset factor were determined using the test module. Evaluating correctness entails taking into account the subsequent error situations.

- Nonlinearity in the ADC
- The resistors' tolerance when used
- The precision of the operational amplifiers utilized
- The precision of the LEMs' transducers

An analog-to-digital converter of the successive approximation type with a precision of 10 bits is included inside the ATMEGA 328 micro-processor. The ATMEGA328 controller's datasheet specs state that the error is  $\pm 1$ LSB (Least Significant Bit). As a result, it is found that the used converter has an accuracy of  $\pm 0.125$  %. The following calculations have also been done, assuming that the resistors used in the components have a tolerance of 0.05 %. The instantaneous product value of voltage (V) and current (I) is used to calculate power (P).

$$P = V * I \quad (4)$$

The transducer is powered by the power supply unit, which generates  $\pm 12$ V from a main supply of 230V. There might be a 2 % measurement error in the power supply module. The voltage divider circuit design uses resistor components with a tolerance of 0.06 %. The fact that 0.95V is thought to represent the internal reference voltage is interesting.

Therefore, the total error might be responsible for  $2 + 0.06 \times 2 = 2.12$  % = 0.02014v.

$$V = (0.95 \pm 0.02014) \times \left(1 + \frac{R_{f1}}{R_1}\right) - \left(\frac{R_{f1}}{R_1}\right) \times V_{LEM(v)} \times K_{vi}$$
 The instantaneous voltage and current values acquired from the transducer output, multiplied by the appropriate scaling factor, may be found using the following equation:

Where,  $k_{vi}$  is a voltage scaling factor.

The present measurement is similar to that.

$$I = (0.95 \pm 0.02014) \times \left(1 + \frac{R_{f1}}{R_1}\right) - \left(\frac{R_{f1}}{R_1}\right) \times V_{LEM(v)} \times K_{ii}$$

The current scaling factor is denoted by  $k_{ii}$ .

The ADC error percentage is  $\pm 0.124$  %.

**6.2.3.1. Voltage accuracy measurement.** According to the manufacturer's datasheet, the LEM LV 25P transducer has a secondary coil current percentage error of 0.95 %. The RMS output of the LEM transducer is 1.99V when it receives an input voltage of 230V. The following formula may be used to determine the percentage inaccuracy of  $V_{LEM(v)}$

while taking into account the tolerances of all resistors used in the circuit:

$$V_{LEM(v)} = LEM(er) + R_{fi}(er) + R_1(er) + R_2(er) + R_3(er)$$

Where,  $R_2 = 100 \text{ k}\Omega$ ,  $R_3 = 100\Omega$ .

$$V_{LEM(v)} = 0.95\% + 0.06\% + 0.06\% + 0.06\% + 0.06\% = 1.19\% \text{ of } 1.89\text{v} \\ = 0.023681\text{v}$$

Thus, the equation above may be expressed as,

$$V = (0.95 \pm 0.02014) \times \left(1 + \frac{R_{fi}}{R_1}\right) - \left(\frac{R_{fi}}{R_1}\right) \times V_{LEM(v)} \times K_{vi}$$

$$V = (1.8 \pm 0.0586) \times k_v$$

Consequently, the percentage error in the voltage measurement is  $0.0586 \pm 1.8 = \pm 3.25 \%$ . Thus, the overall percentage error in voltage measurement is  $3.250 + 0.1250 = \pm 3.375 \%$ .

**Current accuracy measurement:** A current transducer, such the LEM LA 25P, can be used to measure the primary current supplied to the load. A load resistor with a resistance of  $100\Omega$  encounters a corresponding secondary current (I) of 2 mA when given a transducer with a nominal current of 2A. An RMS output voltage corresponding to 0.2A is obtained in the LEM transducer with this arrangement. Thus, it is possible to calculate the total % inaccuracy in the present transducer in the following way:

$$V_{LEM(i)} = LEM(er) + R_{fi}(er) + R_1(er) + R_2(er) + R_3(er)$$

Here,  $R_2 = 100000\Omega$ ,  $R_3 = 100\Omega$ .

$$V_{LEM(i)} = 1.06\% \text{ of } 0.2\text{A} = 0.02\text{A}$$

$$I = (0.95 \pm 0.02014) \times \left(1 + \frac{R_{fi}}{R_1}\right) - \left(\frac{R_{fi}}{R_1}\right) \times V_{LEM(v)} \times K_{ii}$$

$$I = (1.8 \pm 0.0407) \times k_i$$

The current measurement error is determined to be  $\pm 2.260 \%$ . When incorporating the ADC error, the total error in current measurement becomes  $2.260 \% + 0.1250 \%$ , signification in a cumulative percentage error of  $\pm 2.3850 \%$ . Consequently, the overall percentage error in power measurement is computed as the sum of the errors in current measurement and ADC, which is  $\pm 5.010 \%$  ( $2.6250 \% + 2.3850 \%$ ).

**Power consumption measurement:** SEM units, operational 24 h a day throughout the entire year, play a significant role in the overall annual electricity consumption. The energy use of the load controllers used in the experiment was examined as well as the SEM unit that was on display in order to mitigate this effect. Table 4 provides an estimate of the power usage for these parts (see Table 5).

### 6.3. Energy monitoring system with Internet of Things environment

To utilize the webpage's functionality, users must input their login credentials on the login screen, which is shown in Fig. 18. Upon successful login, users are granted access to the main page, enabling them to explore and make use of the diverse functionalities available.

Users may choose from a variety of laboratories, watch trend graphs of energy use, obtain power usage statistics, and monitor energy consumption in real time all from the main page. Fig. 19 displays load-wise power information, including RMS current, power demand, power factor, energy consumption, and a load's assigned priority, inside the developed SEMs. The total energy utilized by the selected laboratory will be displayed on a display at the bottom of the page. As seen in Fig. 19, the home page has a facility to display the trend graph illustrating the power consumption of various loads.

## 7. Conclusion

The ISEMS is intended to provide a demand-side energy management platform with a focus on the integration of renewable energy sources. The Smart Energy Management unit's power negotiation algorithms are developed and tested in a controlled laboratory environment by ISEMS, which also performs tests to demonstrate the efficacy of these algorithms. The ISEMS is centered on making the best use of renewable energy sources, especially when there is less available power generation. This optimization is made possible by precise solar irradiation forecasts made both one month and one day in advance. The system successfully lowers the utilization of low-priority, or non-critical appliances. Experiments conducted in real time show that only appliances with higher priorities can operate under demand limit limitations. To create dependable predictive models, a number of machine learning techniques are examined, including ensemble methods, PSO-based SVM, Artificial Neural Networks Support Vector Machines, and Particle Swarm Optimization based ANN. Two metrics are utilized in model comparisons: MAE and Mean Absolute Percentage Error. The PSO-based SVM model works better than earlier models seen in the literature today. The automatic hyper parameter change of the PSO optimization approach is responsible for this benefit.

### CRedit authorship contribution statement

**Challa Krishna Rao:** Writing – review & editing, Writing – original draft, Visualization, Supervision, Resources, Methodology, Formal analysis, Data curation, Conceptualization. **Sarat Kumar Sahoo:** Writing – review & editing, Writing – original draft, Visualization, Validation, Supervision, Methodology, Investigation, Formal analysis, Data curation, Conceptualization. **Franco Fernando Yanine:** Writing – review & editing, Writing – original draft, Visualization, Validation, Supervision, Software, Methodology, Investigation, Funding acquisition, Formal analysis, Data curation, Conceptualization.

### Declaration of Competing interest

- No Conflict for publication
- All authors have participated in (a) conception and design, or analysis and interpretation of the data; (b) drafting the article or revising it critically for important intellectual content; and (c) approval of the final version.
- This manuscript has not been submitted to, nor is under review at, another journal or other publishing venue.
- The authors have no affiliation with any organization with a direct or indirect financial interest in the subject matter discussed in the manuscript

## References

- [1] J.O. Agyemang, D. Yu, J. Kponyo, *Autonomic IoT: towards smart system components with Cognitive IoT*, in: Proceedings of the Pan-African Artificial Intelligence and Smart Systems Conference, Windhoek, Namibia, Springer, Berlin/Heidelberg, Germany, September 2021, pp. 6–8.
- [2] C. Krishna Rao, S.K. Sahoo, F.F. Yanine, *An IoT-based intelligent smart energy monitoring system for solar PV power generation*, in: Energy Harvesting and Systems, 2023. Walter de Gruyter GmbH.
- [3] A.K. Bashir, S. Khan, B. Prabadevi, N. Deepa, W.S. Alnumay, T.R. Gadekallu, P.K. R. Maddikunta, *Comparative analysis of machine learning algorithms for predicting smart grid stability*, *Int. Trans. Electr. Energy Syst.* 31 (2021) e12706.
- [4] H. Bhasin, S. Bhatia, *Application of genetic algorithms in machine learning*, *Int. J. Comput. Sci. Inf. Technol.* 2 (2011) 2412–2415.
- [5] S.F.A. Shah, M. Iqbal, Z. Aziz, T.A. Rana, A. Khalid, Y.N. Cheah, M. Arif, *The role of machine learning and the Internet of things in smart buildings for energy efficiency*, *Appl. Sci.* 12 (2022) 7882.
- [6] M. Mohammadi, T.A. Rashid, S.H.T. Karim, A.H.M. Aldalwie, Q.T. Tho, M. Bidaki, A.M. Rahmani, M. Hosseinzadeh, *A comprehensive survey and taxonomy of the SVM-based intrusion detection systems*, *J. Netw. Comput. Appl.* 178 (2021) 102983.

- [7] M.A. Almaiah, O. Almomani, A. Alsaaidah, S. Al-Otaibi, N. Bani-Hani, A.K. A. Hwaitat, A. Al-Zahrani, A. Lutfi, A.B. Awad, T.H. Aldhyani, Performance investigation of principal component analysis for intrusion detection system using different support vector machine kernels, *Electronics* 11 (2022) 3571.
- [8] M. Balasaraswathi, K. Srinivasan, L. Udayakumar, S. Sivasakthiselvan, M. G. Sumithra, Big data analytics of contexts and cascading tourism for smart city, *Mater. Today: Proc.* (2020).
- [9] C.K. Rao, S.K. Sahoo, F.F. Yanine, A literature review on an IoT-based intelligent smart energy management systems for PV power generation, in: *Hybrid Advances, Elsevier BV*, 2023 100136, <https://doi.org/10.1016/j.hybadv.2023.100136>.
- [10] A. Bashar, M.R. Rabbani, S. Khan, M.A.M. Ali, Data-driven finance: a bibliometric review and scientific mapping, in: *Proceedings of the 2021 International Conference on Data Analytics for Business and Industry (ICDABI)*, 2021, pp. 161–166.
- [11] Firat Bestepe, Sevgi Ozkan Yildirim, Acceptance of IoT-based and sustainability-oriented smart city services: a mixed methods study, *Sustain. Cities Soc.* 80 (2022).
- [12] Kartik Bhardwaj, Krishna, Siddhant Banyal, Deepak Kumar Sharma, Waleed Al-Numay, Internet of things-based smart city design using fog computing and fuzzy logic, *Sustain. Cities Soc.* 79 (2022).
- [13] S. Blasi, A. Ganzaroli, I. De Noni, Smartening sustainable development in cities: strengthening the theoretical linkage between smart cities and SDGs, *Sustain. Cities Soc.* 80 (2022).
- [14] S. Afzal, A. Faisal, I. Siddique, M. Afzal, Internet of things (IoT) security: issues, challenges and solutions, *Int. J. Sci. Eng. Res.* 12 (2021) 52–61.
- [15] M. Raghul, S. Jeevitha, S. Deveswaran, Monitoring maximum power point of photovoltaic systems, *Int. Res. J. Mod. Eng. Technol. Sci.* 4 (2022) 8.
- [16] H. Hamdani, A.B. Pulungan, D.E. Myori, F. Elmubdi, T. Hasannuddin, Real time monitoring system on solar panel orientation control using visual basic, *J. Appl. Eng. Technol. Sci.* 2 (2021) 112–124.
- [17] A.A. Lekvan, R. Habibifar, M. Moradi, M. Khoshjahan, S. Nojavan, K. Jermsttiparsert, Robust optimization of renewable-based multi-energy micro-grid integrated with flexible energy conversion and storage devices, *Sustain. Cities Soc.* 64 (2021) 102532.
- [18] M. Peña, F. Biscarri, E. Personal, C. León, Decision support system to classify and optimize the energy efficiency in smart buildings: a data analytics approach, *Sensors* 22 (2022) 1380.
- [19] K. Piatek, A. Firlit, K. Chmielowiec, M. Dutka, S. Barczeniewicz, Z. Hanzelka, Optimal selection of metering points for power quality measurements in distribution system, *Energies* 14 (2021) 1202.
- [20] P.W.T. Pong, A.M. Annaswamy, B. Kroposki, Y. Zhang, R. Rajagopal, G. Zussman, H.V. Poor, Cyber-Enabled grids: shaping future energy systems, *Adv. Appl. Energy* 1 (2021) 100003.
- [21] Pawar, P., & Vittal K, P. Design and development of advanced smart energy management system integrated with IoT framework in a smart grid environment. In *J. Energy Storage* (Vol. 25, p. 100846). Elsevier BV.
- [22] T. Ahmad, R. Madonski, D. Zhang, C. Huang, A. Mujeeb, Data-driven probabilistic machine learning in sustainable smart energy/smart energy systems: key developments, challenges, and future research opportunities in the context of smart grid paradigm, *Renew. Sustain. Energy Rev.* 160 (2022) 112128.
- [23] H. Zhang, H. Feng, K. Hewage, M. Arashpour, Artificial neural network for predicting building energy performance: a surrogate energy retrofits decision support framework, *Buildings* 12 (2022) 829.
- [24] G. Demirezen, A. Fung, M. Deprez, Development and optimization of artificial neural network algorithms for the predictive of building specific local temperature for HVAC control, *Int. J. Energy Res.* 44 (2020) 8513–8531.
- [25] C.K. Rao, S.K. Sahoo, F.F. Yanine, Demand response for renewable generation in an IoT based intelligent smart energy management system. 2021 *Innovations in Power and Advanced Computing Technologies (I-PACT)*, Kuala Lumpur, Malaysia, 2021, pp. 1–7.
- [26] T. Mazhar, M.A. Malik, I. Haq, I. Rozeela, I. Ullah, M.A. Khan, D. Adhikari, M. T. Ben Othman, H. Hamam, The role of ML, AI, and 5G technology in smart energy and smart building management, *Electronics* 11 (2022) 3960.
- [27] D. Gupta, S. Juneja, A. Nauman, Y. Hamid, I. Ullah, T. Kim, E.M. Tag Eldin, N. A. Ghamry, Energy saving implementation in hydraulic press using industrial Internet of things (IIoT), *Electronics* 11 (2022) 4061.
- [28] R. Khan, Q. Yang, I. Ullah, A.U. Rehman, A.B. Tufail, A. Noor, A. Rehman, K. Cengiz, 3D convolutional neural networks based automatic modulation classification in the presence of channel noise, *IET Commun.* 16 (2022) 497–509.
- [29] M. Raza, A.R. Barkat, A.U. Rehman, A. Rehman, I. Ullah, Mobile crowdsensing based architecture for intelligent traffic predictive and quickest path selection, in: *Proceedings of the 2020 International Conference on UK-China Emerging Technologies (UCET)*, 20–21 August 2020, pp. 1–4. Glasgow, UK.
- [30] G. Lilis, G. Conus, N. Asadi, M. Kayal, Towards the next generation of intelligent building: an assessment study of current automation and future IoT based systems with a proposal for transitional design, *Sustain. Cities Soc.* 28 (2017) 473–481.
- [31] C.K. Rao, S.K. Sahoo, M. Balamurugan, F.F. Yanine, Design of smart socket for monitoring of IoT-based intelligent smart energy management system, in: *Lecture Notes in Electrical Engineering*, Springer, Singapore, 2021, pp. 503–518.
- [32] K.P. Kumar, B. Saravanan, Day-ahead scheduling of generation and storage in a microgrid considering demand Side management, *J. Energy Storage* 21 (June 2018) (2019) 78–86.
- [33] M. Zachar, P. Daoutidis, Energy management and load shaping for commercial microgrids coupled with flexible building environment control, *J. Energy Storage* 16 (2018) 61–75.
- [34] F. Abate, M. Carratù, C. Liguori, V. Paciello, A low-cost smart power meter for IoT, *Measurement* 136 (2019) 59–66.
- [35] F.A. Qureshi, C.N. Jones, Energy & Buildings Hierarchical control of building HVAC system for ancillary services provision, *Energy Build.* 169 (2018) 216–227.
- [36] F. Abate, M. Carratù, C. Liguori, V. Paciello, A low-cost smart power meter for IoT, *Measurement* 136 (2019) 59–66.
- [37] A.H. Alavi, P. Jiao, W.G. Buttlar, N. Lajnef, Internet of things-enabled smart cities: state-of-the-art and future trends, *Measurement* 129 (July) (2018) 589–606.
- [38] C.K. Rao, S.K. Sahoo, M. Balamurugan, S.R. Satapathy, A. Patnaik, F.F. Yanine, Applications of sensors in solar energy systems, in: *2020 International Conference on Renewable Energy Integration into Smart Grids: A Multidisciplinary Approach to Technology Modelling and Simulation (ICREISG)*, 2020. IEEE.
- [39] A.U. Rehman, Z. Wadud, R.M. Elavarasan, G. Hafeez, I. Khan, Z. Shafiq, H. F. Alhelou, An optimal power usage scheduling in a smart grid integrated with renewable energy sources for energy management, *IEEE Access* 9 (2021) 84619–84638.
- [40] P. Pawar, K.P. Vittal, Design of smart socket for power optimization in home energy management system, in: *2nd IEEE International Conference on Recent Trends in Electronics, Information & Communication Technology*, 2017, pp. 1739–1744.
- [41] M. Asif, W.U. Khan, H.R. Afzal, J. Nebhen, I. Ullah, A.U. Rehman, M.K. Kaabar, Reduced-complexity LDPC decoding for next-generation IoT networks, *Wirel. Commun. Mob. Comput.* 2021 (2021) 2029560.
- [42] B.K. Yousafzai, S.A. Khan, T. Rahman, I. Khan, I. Ullah, A. Ur Rehman, M. Baz, H. Hamam, O. Cheikhrouhou, Student-performulator: student academic performance using hybrid deep neural network, *Sustainability* 13 (2021) 9775.
- [43] Z. Xiaoyi, W. Dongling, Z. Yuming, K.B. Manokaran, A.B. AntonyIoT-drive, framework-based efficient green energy management in smart cities using multi-objective distributed dispatching algorithm, *Environ. Impact Assess. Rev.* 88 (2021).
- [44] Yu, L. Deep Reinforcement Learning for Smart Building Energy Management: A Survey. arXiv 2020, arXiv:2008.05074.
- [45] D. Zhang, X. Han, C. Deng, Review on the research and practice of deep learning and reinforcement learning in smart grids, *CSEE J. Power Energy Syst.* 4 (2018) 362–370.
- [46] I.H. Sarker, A. Colman, J. Han, A.I. Khan, Y.B. Abushark, K. Salah, Behavdt: a behavioral decision tree learning to build a user-centric context-aware predictive model, *Mob. Netw. Appl.* 25 (2020) 1151–1161.
- [47] E. Aliyan, M. Aghamohammadi, M. Kia, A. Heidari, M. Shafie-khah, J.P. Catalão, Decision tree analysis to identify harmful contingencies and estimate blackout indices for predicting system vulnerability, *Electr. Power Syst. Res.* 178 (2020) 106036.
- [48] A. Ajitha, Maitri Goel, Mohit Assudani, Sudha Radhika, Sanket Goel, Design and development of residential sector load predictive model during COVID-19 pandemic using LSTM based RNN, *Elec. Power Syst. Res.* 212 (2022) 108635.
- [49] B. Dave, S. Kubler, K. Främling, L. Koskela, Opportunities for enhanced lean construction management using Internet of Things standards, *Int. J. Pervasive Comput. Commun.* 61 (Jan. 2020) 86–97.
- [50] C.K. Rao, S.K. Sahoo, F.F. Yanine, Demand side energy management algorithms integrated with the IoT framework in the PV smart grid system, in: *Advanced Frequency Regulation Strategies in Renewable-Dominated Power Systems*, Elsevier, 2024, pp. 255–277.
- [51] F.H. Shajin, P. Rajesh, Trusted secure geographic routing protocol: outsider attack detection in mobile ad hoc networks by adopting trusted secure geographic routing protocol, *Int. J. Pervasive Comput. Commun.* (Dec. 2020).
- [52] A. Prasanth, S. Jayachitra, A novel multi-objective optimization strategy for enhancing quality of service in IoT-enabled WSN applications, *Peer-to-Peer Networking and Applications* 13 (6) (2020) 1905–1920.
- [53] S.E. Ahmadi, N. Rezaei, H. Khayyam, Energy management system of networked microgrids through optimal reliability-oriented day-ahead self-healing scheduling, *Sustainable Energy, Grids and Networks* 23 (2020) 100387.